Identification of Cascaded Microwave Circuits with Moderate Reflections Using Reflection and Transmission Measurements

TIMO V. VEIJOLA AND MARTTI E. VALTONEN, MEMBER, IEEE

Abstract—**A method for identifying the component values of a cascaded microwave circuit with the aid of the time-domain reflection and transmission coefficients is presented. The model proposed is composed of commensurate nondispersive transmission lines separated by either lumped series or shunt resistances. The line delays are equal to the sampling interval. The algorithm takes into account the third-order multiple reflections, thus allowing identification of circuits with moderate internal reflections (reflection coefficient smaller than about 0.2). The method can be applied to the modelling of connectors, discontinuities, transitions, jigs, and even impedance transformers. A numerical example is given to demonstrate the ability of the algorithm.**

I. Introduction

FINDING THE equivalent circuit of a cascaded (low-pass) microwave structure is often of vital importance. This is the case in, e.g., jig peeling for active device measurements, deriving junction discontinuities, and examining the quality of connectors and transitions. In these types of applications, the reflections are low or moderate (reflection coefficient $\rho < 0.2$) even in the worst case. When the parameters of such circuits are measured in the frequency domain, the results are the most difficult to interpret on a circuit level. The reflection coefficient usually has a large number of ripples in the frequency range of interest. Under these circumstances a rough initial guess for the equivalent circuit and then an optimization for matching the simulated and measured results often unavoidably fail.

A far better insight into the equivalent circuit is obtained if time-domain measurements are used. The recent rapid development of TD instruments for microwaves permits direct TD measurements, and ANA may be used together with FFT. In the traditional TDR techniques (time-domain reflectometer) [1], [2], the reflections due to small impedance steps, nondispersive losses, or discontinuity reactances are observed. If reflections and losses are low, the approximated element values may be found. However, in the case of moderate reflections, multiple reflections distort the results and the identification fails. Megill [3] has presented an algorithm which takes all multiple reflections into account in finding the lossless equivalent circuit composed of impedance steps.

Manuscript received April 22, 1987; revised August 21, 1987.

The authors are with the Circuit Theory Laboratory, Helsinki University of Technology, 02150 Espoo, Finland.

IEEE Log Number 8717978.

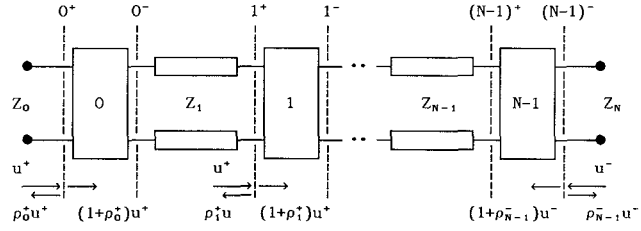

Fig. 1. Two-port model to be identified.

In this paper a new technique is presented, which, in addition to impedance steps, also reveals lumped and distributed series and shunt losses. The algorithm proposed requires both reflection and transmission measurements and takes multiple reflections into account up to the third order. For the identification the circuit is composed of cascaded commensurate dispersionless transmission lines separated by lumped series or shunt resistances (Figs. 1–3). The delay of the lines is equal to the sampling interval.

If only the input reflection coefficient is available, an impedance step can not be distinguished from a series or shunt resistance. However, using the additional information provided by the output reflection and transmission coefficients, a distinction is possible. In the model proposed, the lumped series and shunt resistances as well as impedance steps are seen such as they are. Dispersive losses lead to a model where series resistances (dominating conductor losses) or shunt resistances (dominating dielectric losses) appear repeatedly along the whole length of the line. Serial parasitic inductances and shunt capacitances are seen as short high and low impedance lines, respectively. Shunt inductances and series capacitances are not allowed.

II. Identification of the Two-Port Model

The two-port model to be identified is composed of $N-1$ short lossless transmission lines separated by N lumped loss circuits consisting of either a series or a shunt resistance (Fig. 1). The transmission line delay is equal to the sampling interval (Δt) of the measured signals. The algorithm identifies the transmission line impedances and the loss circuit resistances.

In Fig. 1, ρ_n^+ and ρ_n^-, denoting the *actual* internal reflection coefficients of discontinuity n looking from the

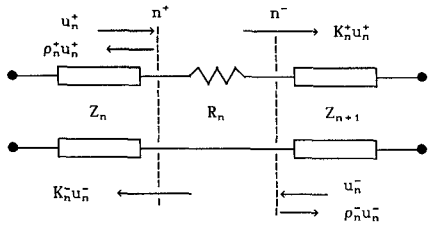

Fig. 2. Loss circuit consisting of a series resistance.

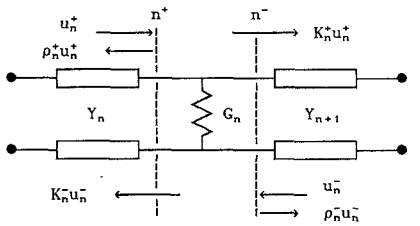

Fig. 3. Loss circuit consisting of a shunt conductance.

left (n^+) and right (n^-), respectively, are given by

$$\rho_n^+ = \frac{R_n + Z_{n+1} - Z_n}{R_n + Z_{n+1} + Z_n} \tag{1}$$

$$\rho_n^- = \frac{R_n + Z_n - Z_{n+1}}{R_n + Z_n + Z_{n+1}} \tag{2}$$

where $n = 0 \cdots N-1$, and Z_0 and Z_N are the termination impedances. The voltage transmission coefficients in the series loss circuit of Fig. 2 are expressed by

$$K_n^+ = \frac{Z_{n+1}}{Z_{n+1} + R_n}\eta_n \tag{3}$$

$$K_n^- = \frac{Z_n}{Z_n + R_n}\eta_n \tag{4}$$

where the first part is due to the voltage divider, and the additional factor η_n takes care of the nondispersive losses. The nondispersive losses are not revealed by reflections, because voltage and current are attenuated in a similar way, thus keeping the driving point resistance constant. However, the measured transmission coefficients together with the transmission coefficients suggested by the model expose the presence of nondispersive losses, as will be seen later in this section.

In the dual case of a shunt conductance (Fig. 3), the line impedances and resistances in (1)–(4) are replaced by admittances and conductances, leading to identical equations for *current* reflection and transmission coefficients.

The transmission coefficient through discontinuity n is equal to $(1+\rho_n^+)K_n^+$ or $(1+\rho_n^-)K_n^-$. Thus the total transmission coefficients of a voltage wave passing through all discontinuities from n to m are the following:

$$T_{n,m}^+ = \prod_{i=n}^{m}(1+\rho_i^+)K_i^+ \tag{5}$$

$$T_{n,m}^- = \prod_{i=n}^{m}(1+\rho_i^-)K_i^-. \tag{6}$$

Using (1)–(4), the total transmission coefficients may also be expressed in the form

$$T_{n,m}^+ = \prod_{i=n}^{m}(1-\rho_i^-)\eta_i \tag{7}$$

$$T_{n,m}^- = \prod_{i=n}^{m}(1-\rho_i^+)\eta_i. \tag{8}$$

In order to determine the component values of the model, the actual reflection coefficients ρ_n^+ and ρ_n^- should be found with the aid of the measured data. An incident voltage wave from port 1 attenuates at discontinuities $0 \cdots n-1$, reflects from discontinuity n, and attenuates again when returning to port 1. The voltage wave from port 2 will attenuate at, respectively, discontinuities $n+1 \cdots N-1$. If the multiple reflections are ignored, the *observed* voltage reflection coefficients originating from discontinuity n (at time $t_n = n2\Delta t$, $t_n' = t_{N-1} - t_n$) can now be written using (7) and (8):

$$\rho_{11}(t_n) = \rho_n^+ T_{0,n-1}^+ T_{0,n-1}^- = \rho_n^+ T_{n-1}^2 \tag{9}$$

$$\rho_{22}(t_n') = \rho_n^- T_{n+1,N-1}^+ T_{n+1,N-1}^- = \rho_n^- \frac{T_{N-1}^2}{T_n^2} \tag{10}$$

where the notation

$$T_n^2 = T_{0,n}^+ T_{0,n}^- = \prod_{i=0}^{n}(1-\rho_i^+)(1-\rho_i^-)\eta_i^2 \tag{11}$$

has been used.

Expressing $T_n^2 = T_{n-1}^2(1-\rho_n^-)(1-\rho_n^+)\eta_n^2$, (9) and (10) yield

$$\rho_n^+ = \frac{\rho_{11}(t_n)}{T_{n-1}^2} \tag{12}$$

$$\rho_n^- = \frac{\rho_{22}(t_n')\eta_n^2\left[T_{n-1}^2 - \rho_{11}(t_n)\right]}{T_{N-1}^2 + \rho_{22}(t_n')\eta_n^2\left[T_{n-1}^2 - \rho_{11}(t_n)\right]} \tag{13}$$

where $T_{-1}^2 = 1$.

After finding the actual internal reflection coefficients, the line impedances and resistances Z_{n+1} and R_n can be solved recursively from (1) and (2):

$$Z_{n+1} = Z_n \frac{1-\rho_n^-}{1-\rho_n^+}, \qquad n = 0 \cdots N-2 \tag{14}$$

$$R_n = Z_n \frac{\rho_n^+ + \rho_n^-}{1-\rho_n^+}, \qquad n = 0 \cdots N-1 \tag{15}$$

provided that $\rho_n^+ + \rho_n^- \geqslant 0$.

If $\rho_n^+ + \rho_n^- < 0$, a dual case is used where (14) and (15) give line admittances Y_{n+1} and shunt conductances G_n when ρ_n^+ and ρ_n^- represent *current* reflection coefficients.

So far, the measured transmission coefficients T_{21} and T_{12} have not explicitly been used. Actually the total delay t_{N-1} in (10) and (13) ($t_n' = t_{N-1} - t_n$) has been identified from T_{21} and T_{12}. In addition, T_{21} and T_{12} are used to reveal the nondispersive loss factors η_n in (13).

The factors η_n can be approximated by comparing the measured two-way transmission coefficient $T_{21}T_{12}$ with the one analyzed from the two-port model (T_{N-1}^2) when $\eta_n = 1$

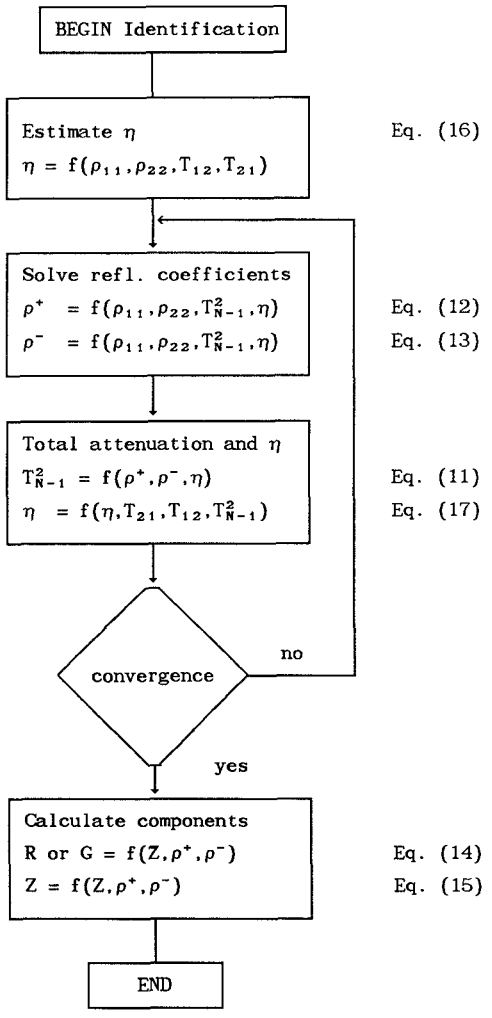

Fig. 4. Identification algorithm.

in (11) and (13). If the nondispersive loss profile along the two-port is known, the magnitude of the losses can be iteratively solved. When the nondispersive attenuation is assumed to be equally distributed along the whole two-port ($\eta_n = \eta$), initial estimate for η may be derived as follows. The actual reflection coefficients ρ_n^+ and ρ_n^- are approximated by $\rho_n^+ = \pm\rho_{11}(t_n)$ and $\rho_n^- = \pm\rho_{22}(t_n')$, where the $-$ sign is used when $\rho_n^+ + \rho_n^- < 0$. These approximations in (11) overestimate the nondispersive losses, and thus the following approximation for η is used:

$$\eta^{(0)} = \left[\frac{T_{21}T_{12}}{\prod_{n=0}^{N-1}\left[\left(1-\left|\rho_{11}(t_n)+\rho_{22}(t_n')\right|+\rho_{11}(t_n)\rho_{22}(t_n')\right)\right]}\right]^{1/4N}. \tag{16}$$

The overestimation has been damped by using $4N$ instead of $2N$ in the exponent. Using this η in (11) repeatedly, the following iterative sequence is obtained:

$$\eta^{(k+1)} = \eta^{(k)}\left[\frac{T_{21}T_{12}}{\left(T_{N-1}^2\right)^k}\right]^{1/2N}. \tag{17}$$

The algorithm is shown in Fig. 4 as a flow diagram.

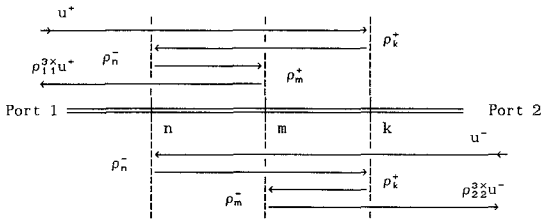

Fig. 5. Multiple third-order reflections.

III. Eliminating the Effect of Third-Order Multiple Reflections

The model outlined in Section II is already satisfactory for the case of low internal reflections. However, if moderate reflections ($\rho < 0.2$) occur, multiple reflections between the discontinuities will lead to erroneous identification. An algorithm for eliminating the third-order reflections from the reflection coefficients is presented in this section.

The model of Fig. 1 suggests the third-order reflections ($\rho^{3\times}$) as shown in Fig. 5. With the aid of this figure a recursive formula is created to express the contribution of multiple reflections to the measured coefficients. After removing the contribution from the measured data, the identification algorithm presented in Section II is applicable. The order of the removed multiple reflections is restricted to 3 due to the exponential increase in computation time as a function of the order.

In Fig. 5 the voltage wave u^+ incident from port 1 reflects between discontinuities n, m and k ($n < m \leqslant k$), and the reflected wave $\rho_{11}^{3\times}(t_r)u^+$ returns at instant t_r, looking like a single reflection from discontinuity $r = m - n + k$:

$$\rho_{11}^{3\times}(t_r) = T_{0,k-1}^+\rho_k^+T_{n+1,k-1}^-\rho_n^-T_{n+1,m-1}^+\rho_m^+T_{0,m-1}^-. \tag{18}$$

Using the identity

$$T_{n+1,k-1}^-T_{n+1,m-1}^+ = \frac{T_{0,k-1}^-}{T_{0,n}^-}\frac{T_{0,m-1}^+}{T_{0,n}^+} \tag{19}$$

eq. (18) can be expressed as a function of the *observed* reflection and transmission coefficients:

$$\rho_{11}^{3\times}(t_r) = A\rho_{11}(t_k)\rho_{11}(t_m)\rho_{22}(t_n')\frac{1}{T_{21}T_{12}} \tag{20}$$

where

$$k = 1\cdots N-1$$
$$m = 1\cdots k$$
$$n = 0\cdots m-1.$$

In (20), substitution $T_{21}T_{12} = T_{N-1}^2$ has been used. If $m = k$, the reflection will occur twice between m and k ($A = 1$). If $m \neq k$, the signal has two paths to propagate between the two discontinuities ($A = 2$).

When looking from port 2, the reflection coefficient $\rho_{22}^{3\times}(t_r')$ at $t_r' = t_{N-1} - t_r$ can be written in a similar way:

$$\rho_{22}^{3\times}(t_r') = A\rho_{22}(t_n')\rho_{22}(t_m')\rho_{11}(t_k)\frac{1}{T_{21}T_{12}} \tag{21}$$

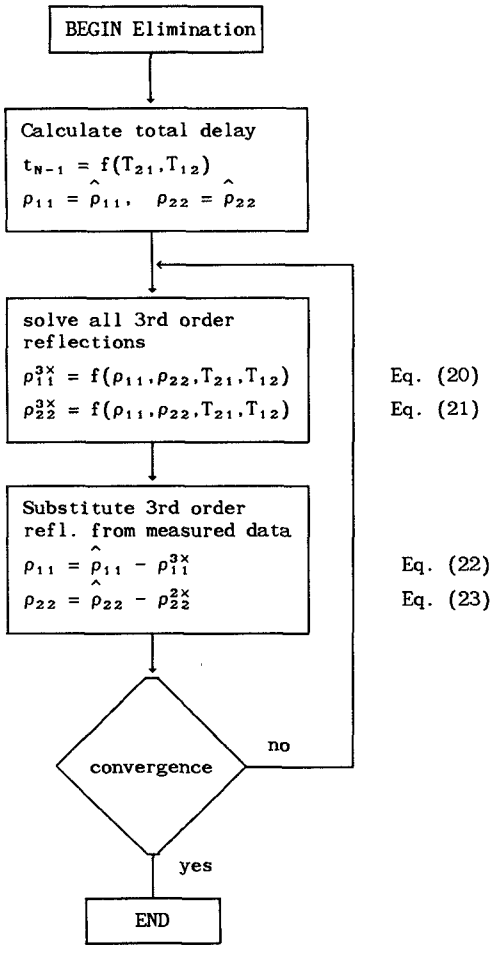

Fig. 6. Algorithm for third-order multiple reflection elimination.

where

$$r = n + m - k$$

and

$$\begin{aligned} n &= 0 \cdots N-2 \\ m &= n \cdots N-2 \\ k &= m+1 \cdots N-1 \end{aligned}$$

and

$$\begin{aligned} A &= 1 \quad \text{if } n = m \\ A &= 2 \quad \text{if } n \neq m. \end{aligned}$$

Note that in (20) and (21) the observed reflection coefficients do not yet include the effect of multiple reflections. This leads to an iterative approach where the observed coefficients must first be estimated. The natural initial estimates for the *observed* coefficients $\rho_{11}(t)$ and $\rho_{22}(t)$ are the *measured* coefficients $\hat{\rho}_{11}(t)$ and $\hat{\rho}_{22}(t)$, respectively.

After summing the multiple reflections at every t_r, they are subtracted from the measured reflection coefficients:

$$\rho_{11}(t_r) = \hat{\rho}_{11}(t_r) - \sum_r \rho_{11}^{3\times}(t_r) \tag{22}$$

$$\rho_{22}(t_r') = \hat{\rho}_{22}(t_r') - \sum_r \rho_{22}^{3\times}(t_r') \tag{23}$$

where $r = 2 \cdots N-1$.

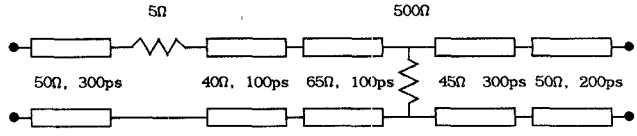

Fig. 7. Circuit of the numerical example.

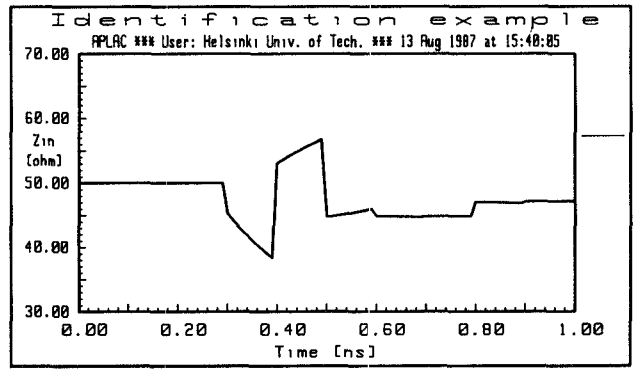

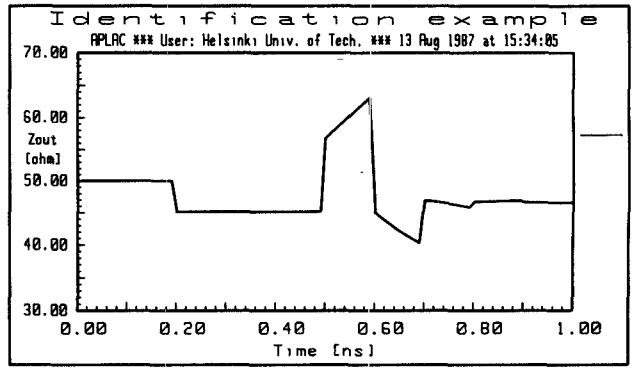

Fig. 8. Impedance profiles seen by the reflectometer.

The algorithm is straightforward but requires a large number of floating point operations if N is large (>100). If all possible third-order reflections are solved, the number of points to be calculated in (20) and (21) is

$$2 \sum_{k=1}^{N-1} \sum_{i=1}^{k} i = \frac{1}{3}(N^3 - N). \tag{24}$$

It should be emphasized that the algorithm given in this section is apart from the identification given in Section II. The algorithm of (22) and (23) only manipulates the measured data, which then can be used as an input for the modeling algorithm.

The algorithm is shown in Fig. 6 as a flow diagram.

IV. Numerical Example

In order to demonstrate the algorithm, the circuit of Fig. 7 was analyzed in the time domain using microwave circuit design tool APLAC [4]. The circuit consists of three nondispersive and two dispersive transmission lines (40-Ω and 65-Ω lines have distributed parallel and series loss, respectively) and two lumped loss resistances. The total delay of the circuit is 1 ns and the total equally distributed nondispersive attenuation of the circuit is 1 dB. The sample interval is 5 ps ($N-1=100$).

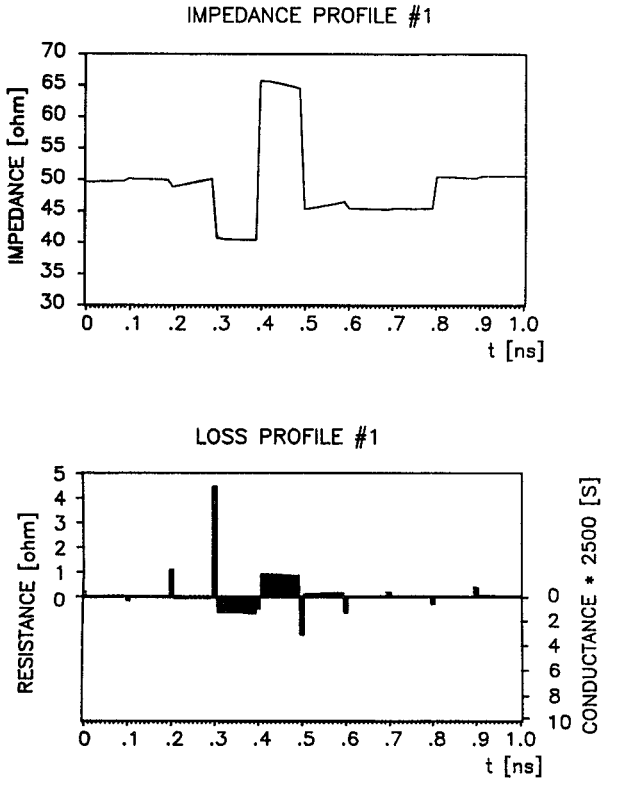

Fig. 9. Impedance and loss profiles without multiple reflection elimination and nondispersive loss iteration.

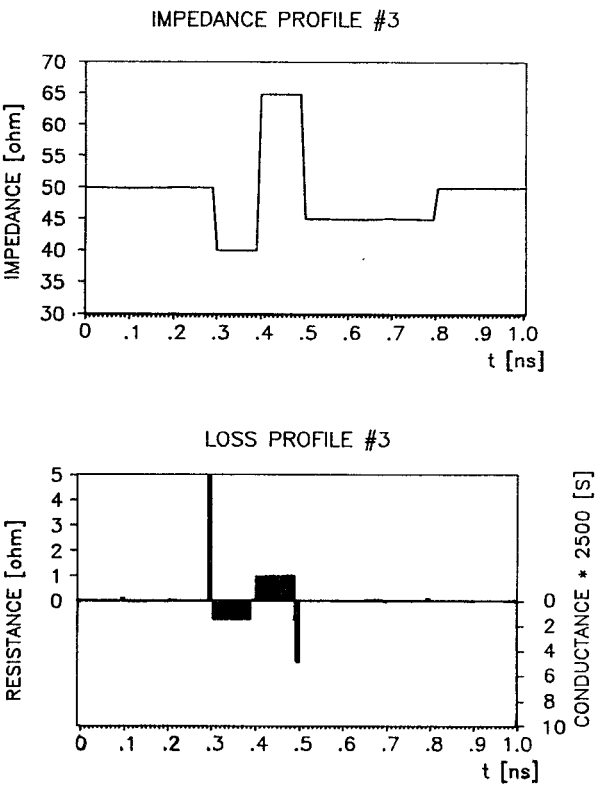

Fig. 11. Final impedance and loss profiles.

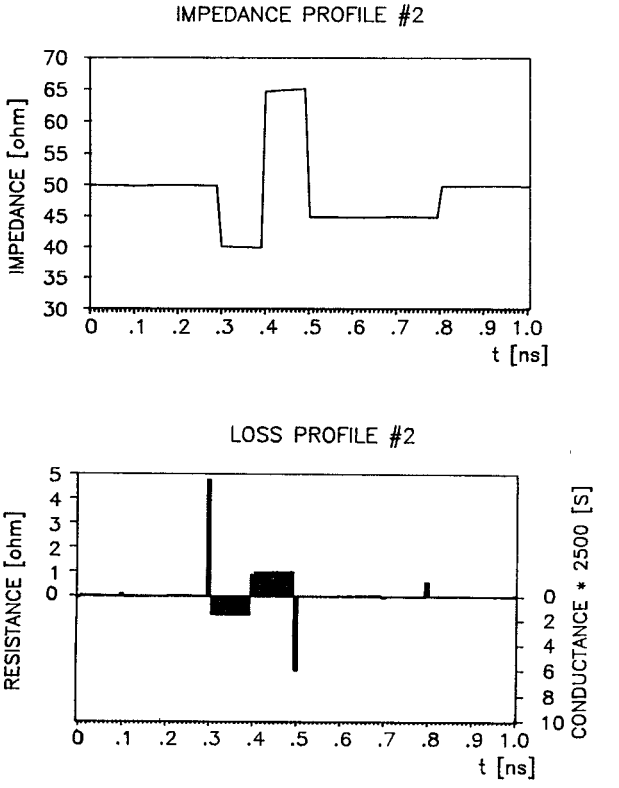

Fig. 10. Impedance and loss profiles without nondispersive loss iteration.

The reflected voltages from the input and output ports of the circuit are transformed to impedances and are plotted in Fig. 8 as seen by a normal reflectometer. The transmission coefficients are $T_{21} = T_{12} = 0.6370$.

Three identifications are made to demonstrate the effect of the multiple reflection elimination and nondispersive attenuation solution. Impedance and loss profiles without multiple reflection elimination and nondispersive loss iteration (algorithm of Fig. 4, $\eta = 1$) are plotted in Fig. 9. In the profiles of Fig. 10, the elimination algorithm of Fig. 6 was used before the identification ($\eta = 1$). The multiple reflections were solved and removed 12 times for complete convergence.

In the final identification (Fig. 11), the total nondispersive transmission coefficient was first estimated by (16) ($\eta^N = -1.196$ dB) and the algorithm illustrated in Fig. 4 was then used. Ten iterations were needed to solve the factor η ($\eta^N = -0.868$ dB). The maximum impedance, resistance, and conductance errors were 0.175 Ω, 0.072 Ω, and $0.108/(50 \cdot 50\ \Omega)$, respectively.

V. Conclusions

A new method to identify cascaded microwave circuits using time-domain reflection and transmission measurements was outlined. All third-order multiple reflections were taken into account. For lossy circuits the algorithm proposed proved to be superior to the traditional TDR techniques when moderate internal reflections ($\rho < 0.2$) occur. This was seen clearly in the numerical example given in Section IV. In Fig. 8 the impedance profiles were

shown as seen by the reflectometer, whereas in Fig. 11 the correct profiles yielded by the new method were illustrated. In addition to impedance profiles the algorithm also produces profiles of lumped as well as distributed dispersive losses (see Fig. 11).

Due to band-limiting effects of the measurement system and frequency-dependent loss, the real values of parasitic reactances may only be roughly estimated. However, matching the identified and measured results in the time domain using, e.g., APLAC, gives the final correct component values.

The method requires the reflection and transmission coefficients in the time domain, but frequency-domain measurements together with FFT may also be used. The algorithm and the Fourier transform utilities are implemented in the automatic network analyzer (HP 8409CT) measurement program ANA-TDR [5], which is written in HP 9000 series 200/300 BASIC.

References

[1] D. Dytting, "Let time domain response provide additional insight into network behavior," presented at RF & Microwave Symp. and Exhibition, Hewlett-Packard.

[2] *Time Domain Reflectometry*, Hewlett-Packard, Application Note 62, 1964.

[3] N. D. Megill, "TDRs profile impedances of backplanes and PC boards," *Electron.*, pp. 113–117, July 14, 1981.

[4] M. Valtonen and T. Veijola, "APLAC—A microcomputer tool especially suited for microwave circuit design in frequency and time domain," in *Proc. XII URSI Nat. Convention Radio Sci.*, 1986, p. 20.

[5] T. Veijola, "Modelling and time domain analysis of lumped and distributed circuits," Licentiate thesis, Helsinki University of Technology, 1986 (in Finnish).

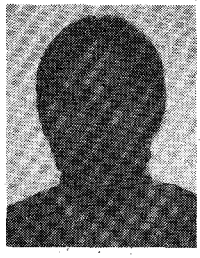

Timo V. Veijola was born in Helsinki on February 4, 1954. He received the Diploma Engineer (M.SC) and the Licentiate of technology degrees in electrical engineering from the Helsinki University of Technology, Finland, in 1980 and 1986, respectively.

Since 1981 he has been working as a Head Engineer in the Circuit Theory Laboratory and in the Laboratory of Metrology at the Helsinki University of Technology. His current research interests are computer aided circuit simulation and modeling, both in frequency and time domain, together with automated network analyzers.

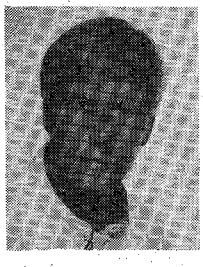

Martti E. Valtonen (S'70–M'73) was born in Helsinki, Finland, on February 7, 1947. He received the degrees of Dipl. Eng., Lic. Tech., and Dr. Tech. in 1970, 1972, and 1975, respectively, all in electrical engineering from the Helsinki University of Technology, Espoo, Finland.

Since 1982, he has been a Professor of Electrical Engineering at the Helsinki University of Technology, engaged in teaching and research of circuit theory and CAD, as well as in teaching of basic electromagnetics. From 1978 to 1979 he was a Research Fellow at the Twente University of Technology, Enschede, The Netherlands, where he worked on microwave CAD and broad-band FET amplifier design. His current research activities involve computer-aided microwave circuit design with special attention to component modeling for time-domain simulation. He is the main author of APLAC microcomputer software for (microwave) circuit design, both in frequency and time domain.

Dr. Valtonen is a member of STS, the Finnish Engineering Society, and EIS, the Finnish Electronics Engineering Society.